The Rheology of Suspensions Containing Polymerically Stabilized Particles

The non-Newtonian viscosities of polymerically stabilized colloidal suspensions are usually predicted and correlated on the basis of data and scaling principles for Brownian hard spheres. Here, the specific effect of the stabilizer layer is investigated using suspensions of monodisperse PMMA particles with a chemically attached stabilizer layer. The ratio between particle radius and stabilizer layer thickness is changed between 5 and 61. At high values of this ratio the data show Brownian hard sphere behavior. At lower values deviations appear. As a first approximation, the "softness" of the particles can be characterized through the concentration at maximum packing. A more detailed comparison with hard sphere data provides a measure for softness that changes with concentration and shear rate. A theoretical estimate of the concentration effect is in line with the experiments. The critical shear stress (or Peclet number) is not a constant but goes through a maximum when the concentration is increased.

Jan Mewis
William J. Frith
Department of Chemical Engineering
Katholieke Universiteit Leuven
Leuven 3030, Belgium

Trevor A. Strivens
I.C.I. Paints Division
Slough, England

William B. Russel
Department of Chemical Engineering
Princeton University
Princeton, NJ

Introduction

Colloidal suspensions are widely used in various industries. In a number of applications, exemplified by materials processing operations, they must be formulated to display a well-defined flow behavior. Coatings, clays and ceramics, electronic pastes, and even food products, all illustrate this problem. Efficient formulation requires that the basic rules governing the rheological behavior of such systems be known. *Ab initio* calculations for nondilute suspensions are only now becoming available. Progress is being made in the simulation of concentrated systems with accurate hydrodynamics (Brady and Bossis, 1984), albeit in two dimensions. At the same time, nonequilibrium statistical mechanics calculations with less refined hydrodynamics suggest the effects of thermodynamic interactions on the structure and the stresses for colloidal suspensions (Russel and Gast, 1986). The results of both approaches bear strong resemblance to predictions from molecular dynamics simulations with no viscous effects (Woodcock, 1984). At this stage the available results are not yet of immediate utility in solving engineering problems.

Lacking fundamental calculations, predictions can still be made by combining suitable scaling principles with adequate yardstick experiments. Krieger (1963) has suggested such a procedure for Brownian hard spheres, that is, stable hard spheres with Brownian motion but without long-range interparticle forces. In systems of practical interest, attractive and repulsive forces contribute significantly to the overall behavior and must be taken into account. Thus scaling laws for electrostatic and/or polymeric (steric) repulsion must be developed.

As a first approximation, polymerically stabilized systems are assumed to have a rigid stabilizer layer. This leads to the definition of an effective volume fraction, which includes the core volume as well as the stabilizer layer. Using this effective volume, the scaling rules for hard spheres apply (Krieger, 1972). The approach succeeds in dilute systems, but in more concentrated suspensions the hydrodynamic and thermodynamic interactions generally deform the stabilizer layer. Such deformations can be detected in osmotic pressure experiments (Cairns et al., 1981) or measured directly using the Israelachvili technique (Hadziioannou et al., 1986). The effect of stabilizer layer deformability on the rheology has not been investigated systematically. It is the objective of this work to quantify the deviations from hard sphere behavior for polymerically stabilized suspensions as a function of the softness of the repulsion.

Viscosity curves have been measured over a wide concentration range and at several temperatures for particles with different degrees of softness. The curves typically show regions of limiting Newtonian behavior at high and low shear rates, separated by a shear thinning region. At the highest concentrations

Correspondence concerning this paper should be addressed to Jan Mewis.
The present address of W.J. Frith is I.C.I. Corporate Laboratories, Runcorn, UK.

an apparent yield stress develops, resulting in very high relative viscosities at low shear rates (on the order of 10^7). For low degrees of softness the data approach the known results for Brownian hard spheres. With softer particles only a slight change in the inherent shape of the viscosity curves can be noticed. However, the absolute values drop considerably below the hard sphere results. This difference grows larger with increasing concentration and increasing shear rate, as could be expected.

The limiting Newtonian viscosities at high and low shear rates can be used to characterize the softness of the stabilizer layer. If these viscosities are plotted against volume fraction, the curves tend to infinity at a maximum packing. The values of these limiting volume fractions at high and low shear provide a suitable measure for particle softness. In principle the softness should depend on temperature and the medium. In the present case the temperature reduction obeys the hard sphere scaling relations. The position of the transition between the Newtonian plateaus can be characterized by a critical value of the scaled shear stress. It first increases with concentration, up to volume fractions of 0.50, and then decreases toward zero. The data are qualitatively similar to recent results on Brownian hard spheres (de Kruif et al., 1985), although shifted to lower stress levels. There is some theoretical support for the initial increase but not for the subsequent decrease.

Experimental Method

To generate data useful for comparison with theoretical results, it is imperative to have a well-characterized system. The system used here consists of poly(methylmethacrylate) (PMMA) particles suspended in two different hydrocarbon media, decalin (η = 2.76 mPa · s, ρ = 886 kg · m^{-3} at 293 K) and Exsol D200/240 (from Essochem; η = 1.60 mPa · s, ρ = 783 kg · m^{-3} at 293 K). The latter is a hydrogenated high-boiling hydrocarbon fraction. The particles are stabilized by means of grafted poly(12-hydroxystearic acid) chains, with a degree of polymerization of 5. The preparation of the particles is described in the literature (Barrett, 1975; Cairns et al., 1976). One of the reasons for selecting this system is that its properties and microstructure have been studied extensively (Cairns et al., 1976, 1981; Cebula et al., 1983; Pusey and van Megen, 1986).

The particles were synthesized in a mixture of hexane and Exsol and purified by repeated centrifugation and redispersion in the desired medium. Infrared spectroscopy was used to detect residual stabilizer in the medium. The final samples always contained less than 0.2% by weight of free stabilizer. Samples were prepared at volume fractions from 0.01 up to the maximum obtainable by centrifugation.

The size of the PMMA core particle is determined using transmission electron microscopy. The concentration is derived from drying a sample of known weight and calculating the PMMA core volume fraction from the weight fraction. The volume occupied by the stabilizer barrier can be derived by comparing the hydrodynamic or effective volume with the core volume (Krieger, 1972). For this purpose, the viscosities of dilute suspensions are measured with a capillary viscometer. The ratio of the measured value for the intrinsic viscosity to the Einstein value of 2.5 then gives a correction factor f for the volume fraction and also a corrected particle radius. The geometrical characteristics of the particles are given in Table 1. The stabilizer barrier thickness, 9 ± 1 nm, compares well with published data for similar systems (Cairns et al., 1981).

Table 1. Geometrical Characteristics of Particles

Avg. Dia. nm	Coeff. of Vol. Variation %	Ratio	Stabilizer Layer Thickness nm	Barrier/Radius Ratio
84	17	1.74	9	5
475	13	1.10	8	30
1,220	7	1.05	10	61

The rheological measurements were performed on a Weissenberg rheogoniometer R18 and a Rheometrics mechanical spectrometer 705F with both parallel-plate and cone-and-plate geometries. The exposed free surface of the sample was covered with water to avoid evaporation of the medium. In this manner a sample could be kept in the instrument, if necessary, for several days without an appreciable change in properties.

Results for Large Particles

First, the results for the 475 and 1,220 nm particles, with relatively thin stabilizer layers, are discussed. The deviations from hard sphere behavior should be rather minor for these systems. Data for a single particle size and temperature, Figure 1, illustrate the ranges of viscosity and shear rate that are covered. At low to moderate concentrations Newtonian plateaus at high and low shear rates are evident. At the highest concentrations the viscosity appears to diverge in the low shear limit, corresponding to an apparent yield stress. Relative viscosities up to 10^8 have been recorded in this region.

Our first attempt at data reduction consisted of scaling as for Brownian hard spheres. Plotting the relative viscosity against a dimensionless shear rate or Peclet number scales the convection or viscous forces, induced by the applied flow, with Brownian

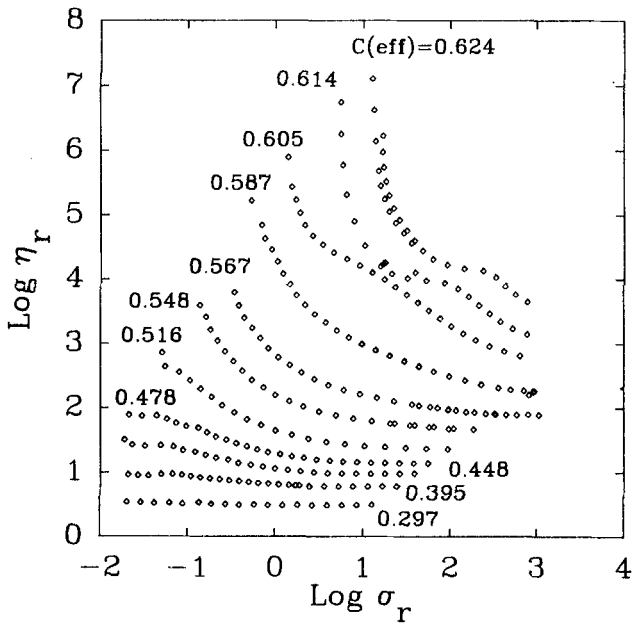

Figure 1. Range of suspension viscosities.
475 nm particles in decalin, T = 293 K

motion. For a dilute suspension the ratio can be expressed by (Krieger, 1963):

$$Pe = \eta_m \dot{\gamma} a^3 / kT \tag{1}$$

where η_m is the viscosity of the medium, $\dot{\gamma}$ is the shear rate, and a is the particle radius. In a nondilute system the medium viscosity does not satisfactorily account for the hydrodynamic interaction between particles. Krieger and Dougherty (1959) suggested using the suspension viscosity η to reflect this increased resistance, assuming in effect that the diffusion of a particle is governed by the suspension viscosity. The resulting Peclet number is essentially a dimensionless or reduced shear stress σ_r:

$$\sigma_r = \eta \dot{\gamma} a^3 / kT \tag{2}$$

The data for suspensions of Brownian hard spheres with the same effective volume fraction c_{eff}, but for different media, temperatures, and particle sizes, should all coincide in this representation. The scaling for temperature works up to moderate concentrations, Figure 2, but fails at volume fractions above 0.50. This can be shown to result from minor changes in volume fraction with temperature, owing to the different thermal expansion coefficients of the particle and the medium (Frith et al., 1987). Proper correction provides a set of consistent results but with volume fractions that depend on temperature. At the highest volume fractions the zero shear Newtonian limit seems to disappear and be replaced by an apparent yield stress. At the same time the viscosity curves change in shape. These features have been discussed elsewhere (Frith et al., 1987).

The fact that the hard sphere scaling applies does not necessarily imply that the particles are really hard spheres. The data should also be compared with available results for hard spheres. This can be done most effectively by comparing the concentration dependence of the limiting Newtonian viscosities at high and low shear. These parameters were obtained by fitting the viscosity–shear stress curves to the semiempirical Krieger-Dougherty (1959) equation:

$$\eta_r = \eta_{r\infty} + \frac{\eta_{ro} - \eta_{r\infty}}{1 + b\sigma_r} \tag{3}$$

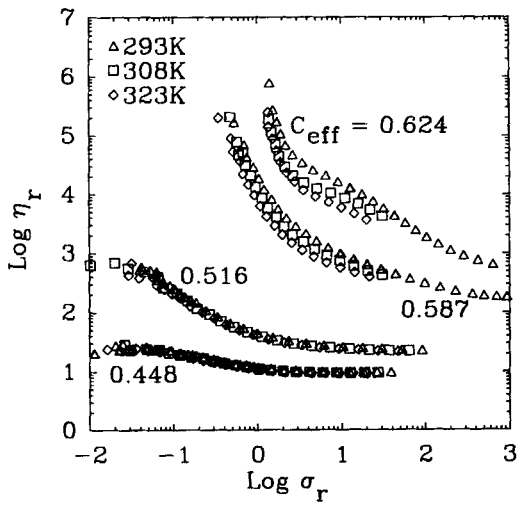

Figure 2. Scaling for Brownian hard spheres applied to temperature effects.
475 nm particles in decalin
△ T = 293 K; □ T = 300 K; ◇ T = 323 K

Recall that according to Eq. 2 the shear rate scales with the inverse third power of the particle radius. Therefore the actual range of shear rates in which the shear thinning occurs depends strongly on particle size. Indeed the zero shear limit was not accessible with the present equipment for the 1,220 nm particles. The limiting viscosities at high and low shear, as derived from Eq. 3 were fitted to a modified version of Mooney's equation, initially suggested by Krieger and Dougherty (1959) and later applied and adapted by various authors (Wildemuth and Williams, 1984):

$$\eta_r = (1 - c/c_m)^{(-[\eta]c_m)} \tag{4}$$

where c is the volume fraction and c_m is the volume fraction at which the viscosity diverges.

Concentrated suspensions of the larger particles are especially susceptible to shear thickening at high shear rates. This makes the determination of η_∞ difficult or even impossible at the highest concentrations. The best estimates of the limiting Newtonian viscosities at high (η_∞) and low (η_o) shear are given in Figures 3a and 3b, respectively, together with the results for the 84 nm particles which will be discussed below.

The limiting high shear data for 1,220 and 475 nm particles superimpose, suggesting hard sphere behavior. The scaling also reduces the data for the 1,220 nm particles in decalin and Exsol to a single curve. However the data lie somewhat above the literature results for Brownian hard spheres (Papir and Krieger, 1970; de Kruif et al., 1985). This discrepancy is even more pronounced for the low shear limit, Figure 3a, although the present data compare well with some previous results on polymerically stabilized systems (Choi and Krieger, 1986). It is not certain at this stage whether the observed behavior should be attributed to residual attractive forces between the particles or to limitations in the concept of the hydrodynamic stabilizer layer thickness. Weak attraction effects should disappear at high stress levels, which is not the case for the observed effect.

It should not be surprising that the effective particle radius, as measured hydrodynamically in a dilute system, does not characterize particle interactions in concentrated suspensions. In the latter case the detailed shape of the interparticle potential should be taken into account. Using Eq. 4, a value for the maximum packing fraction can be calculated from the measured limiting viscosities. Values of 0.49 and 0.62 are obtained, respectively, for limiting low and high shear rates. For Brownian hard spheres the corresponding values were 0.63 and 0.71 (de Kruif et al., 1985). Somewhat higher values were given for a sterically stabilized system by Papir and Krieger (1970): 0.57 and 0.68. De Kruif et al. also found a discrepancy between the capillary measurements on dilute suspensions and the viscosity data on more concentrated systems. However, in their case this seems rather to reflect the difficulties involved in producing well-characterized model suspensions.

Results for Small Particles

The suspensions with 84 nm particles, Table 1, deviate drastically in behavior from those containing larger particles. The lim-

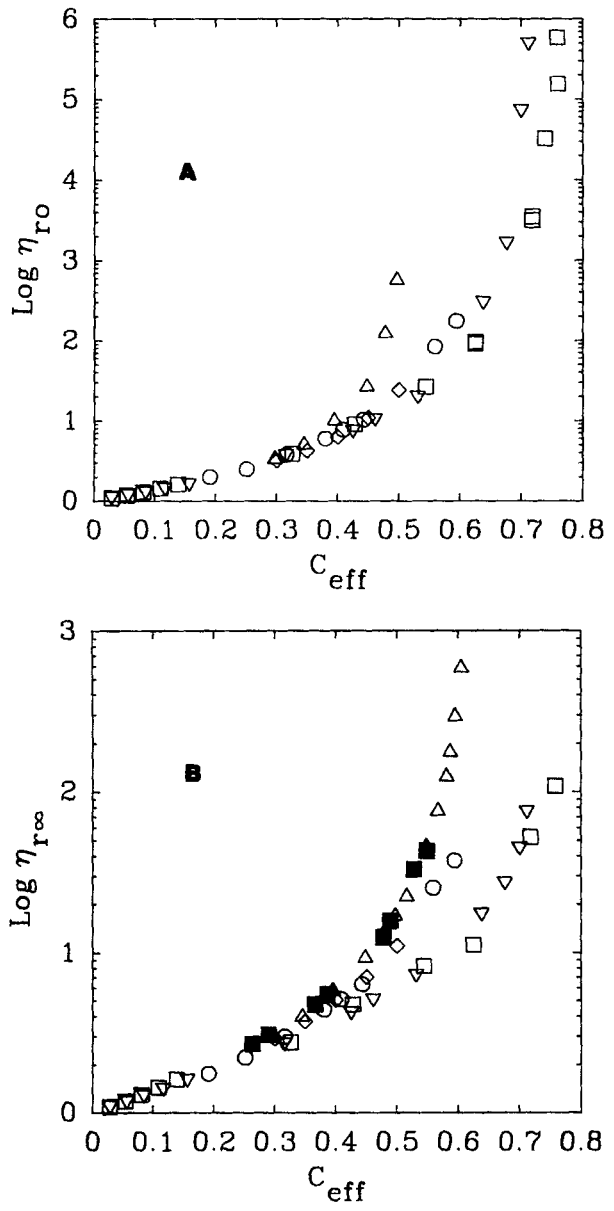

(a) Low shear viscosities;
(b) high shear viscosities.

Figure 3. Limiting shear viscosities compared with published hard sphere results.

o de Kruif et al. (1985); ▽ 84 nm in decalin; □ 84 nm in Exsol; △ 475 nm in decalin; ■ 1,220 nm in decalin; ◇ Papir and Krieger (1970)

iting high and low shear viscosities for the small particles in Figure 3 fall well below the curves for the larger particles. Fitting the data to Eq. 4 gives maximum packing fractions of 0.72 and 0.96, respectively, at low and high shear rates, as compared with 0.49 and 0.62 for the larger particles. The value for high shear rates clearly lies beyond the range possible for hard spheres, but the corresponding core volume fraction (0.55) is still below the hard sphere limit. Hence, the result is physically possible. The data for the two different media are very similar up to volume fractions of 0.60, but diverge somewhat beyond that. At the same time, anomalous effects appear for the dispersions in Exsol

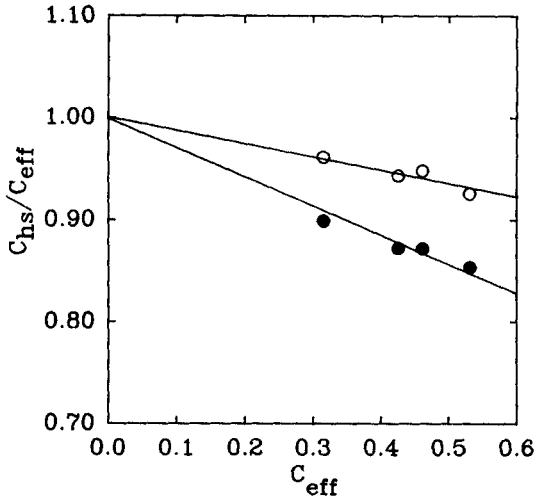

Figure 4. Soft sphere behavior of 84 nm particles, in terms of equivalent hard sphere volume c_{hs}.

o low shear; ● high shear limit

at higher temperatures (Frith et al., 1987). They are not further discussed here.

The volume fraction at maximum packing provides a measure of the particle softness, but describes the complete interparticle potential by only a single parameter. By increasing the concentration and/or shear rate, the stabilizer layer is gradually more compressed, reducing the corresponding effective volume fractions. Information about this phenomenon can be derived from the data by taking, at each concentration and shear rate, the ratio between the effective concentration of the soft spheres and the hard sphere concentration that produces the same viscosity at that shear rate. The result of this exercise is displayed in Figure 4. The ratio does not have to deviate considerably from unity to describe dramatic changes in viscosity, owing to the extreme sensitivity of the latter to concentration. The difference between the concentration ratios in Figure 4 for high and low shear rates is of the order of 10%.

The variation of the effective hard sphere volume fraction c_{eff} with increasing apparent volume fraction can be predicted, or at least rationalized, through a simple perturbation theory. For example, the Gibbs-Bogoliubov inequality (Rasaiah and Stell, 1970) states that the Helmholtz free energy per particle A for a one-component system with pair potential $\Phi(r)$ is bounded by the expression:

$$\frac{A}{kT} \leq \frac{A_{hs}}{kT} + 12c_{eff}\int_1^\infty g_{hs}(x; c_{eff})\frac{\Phi}{kT}x^2\,dx \qquad (5)$$

A_{hs} and g_{hs} are the free energy and radial distribution for a hard sphere system at volume fraction $c_{eff} = \pi D^3 n/6$ with n the number density of spheres. Thus, minimizing the righthand side with respect to the hard sphere diameter D, that is, setting the derivative equal to zero, determines the value of D best representing the system. Use of the thermodynamic expressions relating the radial distribution function and the derivative of the Helmholtz free energy to the osmotic pressure produces:

$$0 = [Z(c_{eff}) - 1]\left[1 - \frac{\Phi(D)}{kT}\right] + 12c_{eff}\int_1^\infty \frac{\partial g_{hs}}{\partial c_{eff}}\frac{\Phi}{kT}x^2\,dx \qquad (6)$$

Values of D can be determined numerically once the interparticle potential Φ, the radius of the bare particle a, and the number density n are specified. Expressions for the compressibility factor Z and g_{hs} are available in the literature.

Recently Milner et al. (1988) derived a simple expression for the interaction potential between terminally anchored layers on flat plates:

$$\frac{\Phi fp}{n_p kT} = \frac{\pi^2}{24}\frac{L^2}{Nl^2}\left[\frac{2L}{h} + 2\left(\frac{h}{2L}\right)^2 - \frac{1}{5}\left(\frac{h}{2L}\right)^5 - \frac{9}{5}\right] \tag{7}$$

for separations $0 \le h \le 2L$

$$L = Nl\left(\frac{12}{\pi^2}\right)^{1/3}\left(\frac{vn_p}{l}\right)^{1/3} \tag{8}$$

relating the layer thickness L to N and l, the number and length of segments in the polymer chain; v/l^3, the excluded volume parameter; and n_p, the surface density of anchored chains. These results apply for highly stretched chains, that is, $L \gg N^{1/2}l$ or $N^{3/2}n_p/l \gg 1$. With the Derjaguin approximation the corresponding potential for interactions between equal spheres follows as:

$$\frac{\Phi}{kT} = \frac{\pi^3}{12} aN^{1/2}ln_p\left(\frac{L}{N^{1/3}l}\right)^3 \cdot \left\{\ln\frac{2L}{h} + \frac{1}{3}\left[1 - \left(\frac{h}{2L}\right)^3\right] - \frac{1}{30}\left[1 - \left(\frac{h}{2L}\right)^6\right] - \frac{9}{5}\left[1 - \frac{h}{2L}\right]\right\} \tag{9}$$

with $h = r - 2a$.

Accurate numerical solutions for D can be obtained from Eqs. 6 and 9 for specified values of the various parameters characterizing the particles and polymer. However, the accuracy of neither the Gibbs-Bologiubov approximation at volume fractions near close packing nor the Derjaguin approximation for polymer layers with $a/L \le 10$ has been tested. In addition, the poly(12-hydroxy stearic acid) chains may be rather short to treat via Eq. 7. For the present, we seek only qualitative results, which can be derived analytically by assuming the layer thickness to be small, $L \ll a$, and the interpenetration of the layers to be even smaller so that $D = 2a + 2L(1 - \epsilon)$ with $\epsilon \ll 1$. Then straightforward expansions lead to:

$$\epsilon = 5\frac{L}{a}\left[\frac{d\ln(Z-1)}{d\ln c_{eff}} - 1\right] \tag{10}$$

for $aN^{1/2}ln_p(L/N^{1/2}l)^3 \gg 1$. The Carnahan-Starling expression for the compressibility factor Z permits the effective volume fractions to be identified explicitly as:

$$c_{HS} = c\left[1 - \frac{15(L/a)^2}{1 + 3L/a}\frac{c(1-c)}{1 - 3c/2 + c^2/2}\right] \tag{11}$$

Here $c = (1 + 3L/a)4\pi a^3 n/3$ refers to the volume fraction deduced from viscosity measurements at infinite dilution.

Figure 5 depicts the predicted variation of the effective volume fraction for the large particles with $L/a = 0.04$ and the small particles with $L/a = 0.2$. As one might expect, the effect is negligible for the former since the layer itself is quite thin. In the latter case the predicted variation is somewhat greater than observed. This may arise from the linearizations required to reduce the result to Eq. 11. Nonetheless, the simple theory demonstrates that crowding of particles at finite volume fractions forces the layers to interpenetrate, thereby reducing the effective hard sphere volume fraction from the value deduced at infinite dilution.

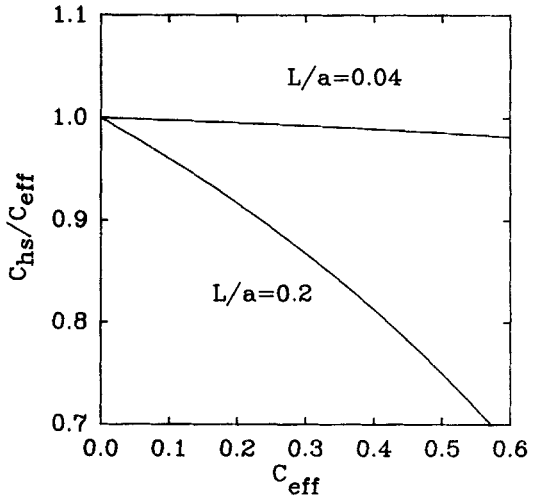

Figure 5. Theoretical estimate of softness effect at low shear rates for 475 and 84 nm particles.

With the small particles a wide range of Peclet numbers can be covered. Thus it becomes possible to investigate the detailed shape of the viscosity curves. Equation 3 contains, except for the limiting viscosities, a factor b. Its inverse, σ_{rc}, can be considered a characteristic relative shear stress, that is, the stress at which the viscosity is exactly halfway between the limiting values. Originally (Papir and Krieger, 1970) σ_{rc} was assumed to be of order unity, regardless of concentration or particle size. De Kruif et al. (1985) recently found a concentration dependence for this parameter in suspensions of silica particles. Their results, obtained on hard spheres, are compared with the present data for the soft 84 nm particles in Figure 6.

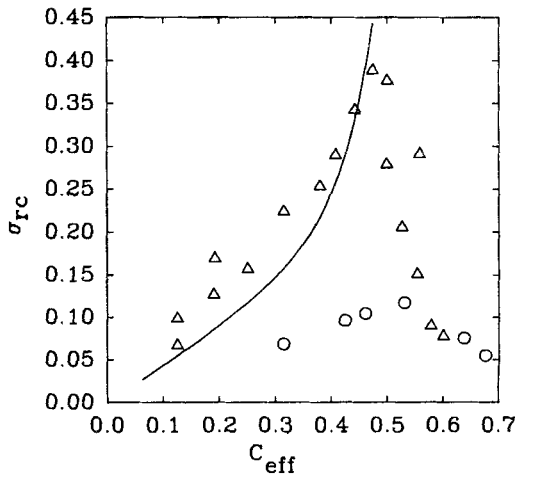

Figure 6. Concentration dependence of σ_{rc}.
Hard sphere data: Δ de Kruif et al. (1985); ○ 84 nm in decalin
—— theoretical estimate.

The shapes of the two experimental curves are qualitatively quite similar, with a maximum at a volume fraction of about 0.50. At this particular concentration hard sphere dispersions undergo a disorder to order transition. However, as with de Kruif's silica particles, our PMMA particles do not show any other rheological transition at the concentration where σ_{rc} has its maximum value. The similarity between the two sets of data indicates that the value of σ_{rc} is not very sensitive to the hardness of the particles. This is contrary to the absolute value of the viscosity at higher volume fractions, which depends strongly on particle softness at higher volume fractions.

A monotonic increase of the factor σ_{rc} with increasing concentration has been predicted theoretically by Russel and Gast (1986). For normal polymer fluids the curves of viscosity vs. shear rate and complex viscosity vs. frequency are often very similar (Cox-Merz analogy). Assuming this analogy to hold for colloidal suspensions, Russel and Gast derived an approximate relation for σ_{rc} from nonequilibrium statistical mechanics calculations of the low shear viscosity and the high frequency modulus. The curve in Figure 6 represents this theoretical estimate, but after multiplication by a factor 5. The calculations are based on a glassy structure that does not necessarily exist at high concentrations, possibly explaining the discrepancy at volume fractions above 0.50.

Equations 3 and 4 suggest the possibility of correlating the viscosity of a given particle-medium system, for various shear rates, temperatures, concentrations, and eventually even particle sizes, by means of a small number of parameters. This requires all the viscosity curves to have the same shape. Especially for soft spheres this seems unlikely. Even for hard spheres one might expect theoretically, and in fact also finds experimentally, an effect of concentration on the intrinsic shape (de Kruif et al., 1985). It can be attributed, at least in part, to a concentration-dependent structure. With the PMMA particles, Eq. 3 works quite well for the 475 nm particles and, up to moderate concentrations, even for the soft 85 nm particles, Table 2.

At high concentrations, the viscosity curves for the 85 nm particles are not well described by Eq. 3. The viscosities tend to change more drastically with shear rate than described by the equation. This results in substantial errors for the limiting viscosities. In these cases better results were obtained with a power law dependence, originally suggested by Cross (1965) for the unscaled viscosity curves of colloidal suspensions:

$$\eta_r = \eta_{r\infty} + \frac{\eta_{ro} - \eta_{r\infty}}{1 + (b\sigma_r)^m} \tag{12}$$

At the highest concentrations for which a zero shear Newtonian limit could still be detected, even this equation fails and the curves must be extrapolated manually to the limiting plateau values. The improvement in curve fitting, resulting from the use of the power m, is illustrated by two cases in Table 2. The gain is more pronounced at the higher concentrations, as can be deduced from the higher values of m, yet the quality of fit is still poor, especially near the end of the curves.

Up to now the shear rate has been scaled in the manner proposed by Krieger (1959), based on the assumption that the suspension viscosity is a direct measure of particle mobility in a concentrated suspension. However the suspension viscosity itself varies with the shear rate and, consequently, provides a rather indirect scaling factor. Using the zero shear viscosity results in a

Table 2. Curve Fitting of Data Using Eqs. 3 and 12

84 nm PMMA Particles in Decalin, T = 293 K					
c_{eff}	η_{ro}	$\eta_{r\infty}$	m	b	Std. Dev. %
0.315	3.61	2.71	1	14.6	1.4
0.425	7.22	4.23	1	10.4	1.5
0.461	10.1	4.9	1	9.6	0.8
0.531	19.6	6.8	1*	8.5	2.4
0.531	19.3	7.3	1.19	8.8	2.1
0.638	342	12.6	1*	20	5.8
0.638	290	17.1	1.29	13.3	1.7
0.676	1,600	27	1.614	18.3	3.27
0.700	7×10^4	44	2.58	26	15.9
0.712	4.8×10^5	74	3.53	23	30.1

*Value of m preset at 1

so-called reduced shear rate $\dot{\gamma}_r$:

$$\dot{\gamma}_r = \frac{\eta_o \dot{\gamma} a^3}{kT} \tag{13}$$

This can be used in conjunction with a viscosity equation similar to Eq. 12:

$$\eta_r = \eta_{r\infty} + \frac{\eta_{ro} - \eta_{r\infty}}{1 + (b'\dot{\gamma}_r)^{m'}} \tag{14}$$

A practical drawback of this method is that the limiting zero shear viscosity is not always accurately known. On the other hand the method results in less steep viscosity curves at high concentrations. Therefore replacing Eq. 12 by Eq. 14 produces a reasonable curve fit up to the highest concentrations where a zero shear viscosity can still be measured, Table 3. The factor m' now actually decreases, rather than increases, at higher concentrations, but the effect is much weaker than in the original data reduction, Table 2. The factor is close to unity for the harder 475 nm particles; the lower values for the 85 nm particles might be related to their softness.

The general shape of the viscosity curves, using the zero shear viscosity as a scaling factor, can be seen in Figure 7. Here, the viscosity is reduced with respect to its upper and lower limits to demonstrate the similarity in shape at different concentrations.

Table 3. Curve Fitting of Data Using Eqs. 13 and 14

84 nm PMMA Particles in Decalin, T = 293 K					
c_{eff}	η_{ro}	$\eta_{r\infty}$	m'	b'	Std. Dev. %
0.315	3.7	2.7	1*	13	1.2
0.425	7.2	4.3	1.15	8.5	1.1
0.461	9.4	4.8	1*	8.3	0.7
0.531	19.5	7.2	0.935	5.9	2.0
0.638	319	15	0.708	8.1	1.7
0.676	1,860	22	0.726	11.4	3.6
0.700	9.2×10^4	31	0.755	21	7.0
0.712	7.0×10^5	46	0.841	15	12

*Value of m' preset at 1

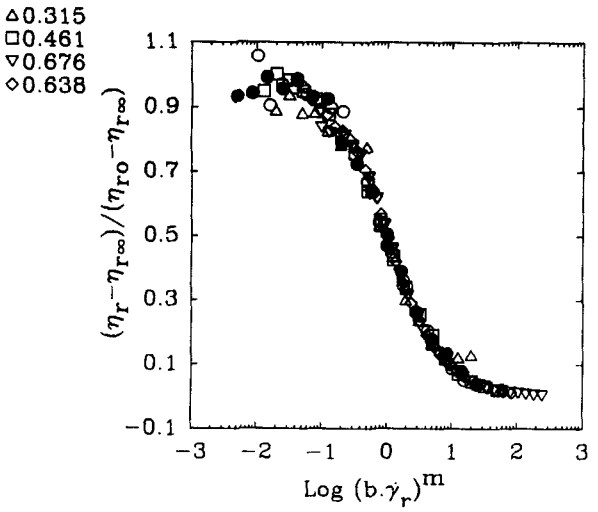

Figure 7. Intrinsic shape of the viscosity curve for soft spheres vs. relative shear rate, Eq. 13.

c_{eff} = 0.32 △; 0.43 ●; 0.46 □; 0.53 ○; 0.64 ◇; 0.68 ▽

Conclusions

Systematic data on the effect of stabilizer layer softness on the rheology of sterically stabilized model colloids are presented. They show that the usual data reduction scheme, based on an effective hard sphere volume fraction, starts to fail if the stabilizer layer becomes sufficiently thick with respect to the particle radius. Even then some of the hard sphere scaling relations hold, for example, for temperature reduction. In the system under consideration, PMMA with poly(hydroxy-stearic acid) as stabilizer grafted on the surface, the transition between hard and soft sphere behavior occurs at ratios of particle radius to stabilizer layer thickness of 5 and 30. The thickness of the stabilizer layer, as calculated from intrinsic viscosity measurements, gives rather low values for the maximum packing. This seems to fit in with some earlier measurements on sterically stabilized dispersions.

The Krieger-Dougherty relation is found to describe well the viscosity-shear rate curves. For the small, soft, particles the curves start to deviate at high concentrations. The curve fitting can be improved by using either an equation suggested by Cross or a relative shear rate rather than a relative shear stress. This last method results in a nearly constant shape for the viscosity curves at all concentrations. As in recent results on hard spheres (de Kruif et al. 1985), the characteristic shear stress is found to change with concentration. The shape of this curve for the soft particles is very similar to that obtained for hard particles, including the downturn at high concentrations. Hence the shape of this curve is rather insensitive to particle hardness.

As a first approximation the particle softness, caused by the deformability of the stabilizer barrier, can be expressed by means of the ratio between the volume fraction at maximum packing for the soft spheres and that for rigid spheres. Comparing the limiting viscosities at high and low shear with those for hard spheres indicates a softness that changes with shear rate and volume fraction. This can be expressed as a shear rate and concentration dependent equivalent hard sphere volume fraction. Owing to the extreme sensitivity, at high volume fractions, of viscosity to concentration, relative changes of 10 to 20% in the equivalent volume fraction describe dramatic changes in viscosity. The experimental result is confirmed qualitatively by a theoretical calculation.

Notation

A = free energy, J
a = particle radius, m
b = constant, Eqs. 3, 12; inverse of characteristic relative shear stress
b' = constant, as b, Eq. 14
c = volume fraction
c_m = concentration at maximum packing
D = effective particle diameter, m
g = radial distribution function
h = particle separation, m
k = Boltzmann's constant, J · K^{-1}
L = layer thickness, m
l = length of polymer segments in a polymer chain, m
m = constant, Eq. 12
N = number of segments in a polymer chain
n_p = surface density of anchored chains, m^{-2}
Pe = Peclet number, Eq. 1
T = absolute temperature, K
v = excluded volume parameter, m^3
Z = compressibility factor

Greek letters

$\dot{\gamma}$ = shear rate, s^{-1}
η = viscosity, Pa · s
σ = shear stress, Pa
Φ = interaction potential, J · m^{-2}

Subscripts

eff = effective
fp = flat plates
hs = hard spheres
m = medium
r = relative
o = zero shear limit
∞ = high shear limit

Literature Cited

Barrett, K. E. J., *Dispersion Polymerization in Organic Media*, Wiley, New York (1975).

Brady, J. F., and G. Bossis, "Dynamic Simulation of Sheared Suspensions. I: General Method," *J. Chem. Phys.*, **80**, 5141 (1984).

Cairns, R. J. R., R. H. Ottewill, D. W. J. Osmond, and I. Wagstaff, "Studies on the Preparation and Properties of Lattices in Nonpolar Media," *J. Colloid Interf. Sci.*, **54**, 45 (1976).

Cairns, R. J. R., W. Van Megen, and R. H. Ottewill, "Comparison between Theoretically Computed and Experimentally Measured Pressures for Interacting Sterically Stabilized Particles," *J. Colloid Interf. Sci.*, **79**, 511 (1981).

Cebula, D. J., J. W. Goodwin, R. H. Ottewill, G. Jenkin, and J. Tabony, "Small-Angle and Quasi-Elastic Neutron Scattering Studies," *Colloid Polym. Sci.*, **261**, 555 (1983).

Choi, G. N., and I. M. Krieger, "Rheological Studies on Sterically Stabilized Dispersions of Uniform Colloidal Spheres. II," *J. Colloid Interf. Sci.*, **113**, 101 (1986).

Cross, M. M., "Rheology of Non-Newtonian Fluids: A New Flow Equation for Pseudoplastic Systems," *J. Colloid Sci.*, **20**, 417 (1965).

de Kruif, C. G., E. M. F. van Iersel, A. Vrij, and W. B. Russel, "Hard Sphere Colloidal Dispersions: Viscosities as a Function of Shear Rate and Volume Fraction," *J. Chem. Phys.*, **83**, 4717 (1985).

Frith, W. J., J. Mewis, and T. A. Strivens, "Rheology of Concentrated Suspensions: Experimental Investigations," *Powder Technol.*, **51**, 27 (1987).

Hadziioannou, G., S. Patel, S. Grannick, and M. Tirrell, "Forces between Surfaces of Block Copolymers Adsorbed on Mica," *J. Am. Chem. Soc.*, **108**, 2871 (1986).

Krieger, I. M., "A Dimensional Approach to Colloid Rheology," *Trans. Soc. Rheol.*, **7**, 101 (1963).

———, "Rheology of Monodisperse Lattices," *Adv. Colloid Interf. Sci.*, **3**, 111 (1972).
Krieger, I. M., and T. J. Dougherty, "A Mechanism for Non-Newtonian Flow in Suspensions of Rigid Spheres," *Trans. Soc. Rheol.*, **3**, 137 (1959).
Milner, S. T., T. A. Witten, and E. Cates, "Theory of the Grafted Polymer Brush," *Phys. Rev. A*, to be published.
Papir, Y. S., and I. M. Krieger, "Rheological Studies on Dispersions of Uniform Colloidal Spheres. II," *J. Colloid Interf. Sci.*, **34**, 126 (1970).
Pusey, P. N., and W. van Megan, "Phase Behavior of Concentrated Suspensions of Nearly Hard Colloidal Spheres," *Nat.*, **320**, 340 (1986).
Rasaiah, J., and G. Stell, "Upper Bounds on Free Energies in Terms of Hard Sphere Results," *Molec. Phys.*, **18**, 249 (1970).
Russel, W. B., and A. P. Gast, "Nonequilibrium Statistical Mechanics of Concentrated Colloidal Dispersions: Hard Spheres in Weak Flows," *J. Chem. Phys.*, **84**, 1815 (1986).
Wildemuth, C. R., and M. C. Williams, "A New Interpretation of Viscosity and Yield Stress in Dense Slurries," *Rheol. Acta*, **23**, 627 (1984).
Woodcock, L. V., "Origins of Shear Dilatancy and Shear Thickening Phenomena," *Chem. Phys. Letters*, **111**, 455 (1984).

Manuscript received June 17, 1988 and revision received Sept. 20, 1988.